2014 European Control Conference (ECC)
June 24-27, 2014. Strasbourg, France

ESC-MRAC of MIMO Systems for Constrained Robotic Motion Tasks in Deformable Environments

Vasiliki Koropouli[1], Azwirman Gusrialdi[2] and Dongheui Lee[3]

Abstract— **Performance of constrained movements in multiple directions of a workspace simultaneously and in presence of uncertainty is a great challenge for robots. Achieving such tasks by employing control policies which are fully determined a priori and do not take into account the system uncertainty can cause undesired stress on the robot end-effector or the environment and result in poor performance. Instead, a sophisticated control policy is required, which can adjust to the varying conditions of a task while taking into account the coupling of motion dynamics between different directions of movement. To this aim, in this paper, we propose a MIMO Extremum Seeking Control (ESC)-Model Reference Adaptive Control (MRAC) approach with the view of executing fine motion tasks in presence of uncertain task dynamics. ESC enhances robustness of the system to non-parametric uncertainties compared to single MRAC. The proposed approach ensures state tracking as well as optimization of a global state-dependent cost criterion in all directions of movement. We evaluate our approach in simulations and in a real-world robotic engraving task.**

I. Introduction

Execution of constrained movements inside unknown and deformable environments is a great challenge for robots due to task uncertainty and the physical coupling of motion dynamics between different directions of movement. Apart from uncertainty, the coupling of motion dynamics has to be taken into account for system modelling and control, see Fig. 1. In this paper, our goal consists of developing a task-space adaptive control approach for accurate performance of multi-directional movements inside unknown and deformable environments.

Performance of constrained robotic motion tasks has been previously investigated by using learning-oriented approaches [1], [2], [3], [4]. In [1], Reinforcement learning is employed, which, however, requires repetitive trials and is not suitable for manipulation of deformable objects where successful execution of a task is required within a single trial to avoid non-desired object deformation caused by many task repetitions. In [2], learned dynamic models are combined with Linear Quadratic Regulator by assuming, however, knowledge of the system dynamics. In [3], an approach for generalizing force control policies to new motion tasks, under different motion-dependent disturbances, is proposed. This method, however, is solely based on demonstrations and does not involve motion feedback.

[1],[3]V. Koropouli and D.Lee are with the Institute of Automatic Control Engineering, Technische Universität München, 80290 München, Germany vicky@tum.de, dhlee@tum.de

[2]A. Gusrialdi is with the Dept. of Electrical Engineering and Computer Science, University of Central Florida, USA Azwirman.Gusrialdi@ucf.edu

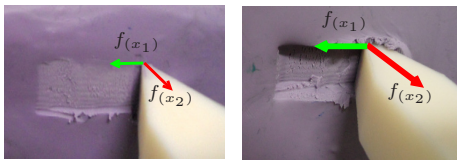

(a) (b)

Fig. 1. An example of a constrained robotic motion task in deformable environment; engraving is realized at different depths inside a plasticine object. Different environmental disturbance $\{f_{(x_1)}, f_{(x_2)}\}$ is experienced in each case due to the changing manipulating mass. Engraving in a (a) low depth, (b) high depth.

The problem of state tracking in presence of uncertainty is treated by traditional Adaptive control [7]. A significant approach is Model Reference Adaptive Control (MRAC) which expresses the ideal behavior of a system in terms of a reference model and makes the system follow the reference model [6]. The use of reference models dates back to the development of aircraft control and, since then, MRAC has been widely used in multiple applications. Recent work on MRAC has been realized in [8], [10], [16]. In [8], a Multiple Input Multiple Output (MIMO) MRAC approach is proposed for output tracking using state feedback. In [10], combination of Extremum Seeking Control (ESC) with MRAC is proposed for state tracking in SISO systems. In [16], an ESC-MRAC approach is proposed for output tracking in nonlinear MIMO systems by performing feedback linearization and the initial problem is converted into output tracking for multiple SISO systems. This method assumes that the control input can be expressed in a specific linear parameterized form. In addition, each SISO system optimizes a cost function which solely depends on this system's output. Although our work deals with state tracking in MIMO systems, the approach in [16] is not recommended for our scenario where we wish that the motion states of different directions of movement track some desired states by simultaneously optimizing a global state-dependent cost in all the directions of movement. This is because task dynamics in different directions are coupled and the controller should not attempt to optimize independently the state tracking error in each direction.

In this work, we propose an ESC-MRAC approach, similar to [10], for state tracking in linear MIMO systems where a global state-dependent cost criterion is optimized in each direction of movement. The ability to express the ideal behavior of a system in terms of a reference model, as in MRAC, is magnificent because the reference model serves in the design of the control law of the system [6]. In addition, MRAC regulates the transient behavior of the system

[10]. However, MRAC lacks robustness to non-parametric uncertainties which are mostly unavoidable in real-world scenarios. In contrast, the combined ESC-MRAC exhibits increased robustness to non-parametric uncertainties since ESC does not rely on the knowledge of the structure of the system dynamics [9], [10], [11].

This paper is structured as follows. First, in Section II, we define the problem, then in Section III we present our proposed ESC-MRAC method and, in Section IV, we evaluate the performance of this method both in simulations and experiments by comparing it with SISO ESC-MRAC [10].

II. Problem formulation

Our goal consists of developing a task-space adaptive control approach for execution of constrained movements in multi-directional workspaces. First, we derive the dynamics of our system and then we define our problem.

A. System modelling

Let us assume an end-effector interacting with an environment in N directions of movement. End-effector motion dynamics can be approximated by the impedance law [12], [13]

$$M_d\ddot{\mathbf{x}} + K_D\dot{\mathbf{x}} + K_P\mathbf{x} = \mathbf{f} - \mathbf{f}_e \tag{1}$$

where $\mathbf{x} \in \mathbb{R}^N$ is end-effector position, $\mathbf{f} \in \mathbb{R}^N$ exerted end-effector force, $\mathbf{f}_e \in \mathbb{R}^N$ the end-effector force which compensates for the environmental disturbance and $M_d \in \mathbb{R}^{N\times N}$, $K_D \in \mathbb{R}^{N\times N}$ and $K_P \in \mathbb{R}^{N\times N}$ are end-effector's inertia, damping and stiffness respectively. At this point, we have to analytically express $\mathbf{f}_e$ to infer the end-effector motion dynamics. Realistic contact is a complex phenomenon and its real modelling is a challenging problem. Instead, the contact force can be expressed by a simple but substantial model as $\mathbf{f}_e = K_e\mathbf{x} + D_e\dot{\mathbf{x}}$ where $K_e \in \mathbb{R}^{N\times N}$ and $D_e \in \mathbb{R}^{N\times N}$ represent the environment's stiffness and damping respectively [14]. The linear form of $\mathbf{f}_e$ preserves the linearity of the interaction law which, in turn, renders system's control design an easier task to achieve, compared to nonlinear systems. We assume isotropic environmental stiffness and damping $K_e = k_eI_N$ and $D_e = d_eI_N$ where I_N is an identity matrix of size N.

First, we analyze the end-effector motion dynamics in a single direction of movement, and then, we generalize to the N-directional workspace. Based on the previous analysis, (1) in the j-th direction can be written as

$$\ddot{x}_j + k_{D_{jj}}\dot{x}_j + k_{P_{jj}}x_j + C(x_l, \dot{x}_l) + (k_ex_j + d_e\dot{x}_j) = f_j \tag{2}$$

where x_j represents end-effector position in the j-th direction and $k_{D_{jj}}$, $k_{P_{jj}}$ are end-effector's damping and stiffness parameters respectively in the j-th direction. The C is a linear function which represents the coupling between the j-th and all $l \in \{1, ..., N\}, l \neq j$ directions. If we substitute end-effector force f_j by a controllable input u_j and expand C to all other $l \neq j$ directions, (2) becomes

$$\ddot{x}_j + k_{D_{jj}}\dot{x}_j + k_{P_{jj}}x_j + \sum_l (k_{D_{jl}}\dot{x}_l + k_{P_{jl}}x_l) + k_ex_j + d_e\dot{x}_j = u_j, \tag{3}$$

where $k_{D_{jj}}$, $k_{D_{jl}}$ are elements of the K_D matrix and $k_{P_{jj}}$, $k_{P_{jl}}$ are elements of the K_P matrix. By applying (3) in all N directions and writing in state-space form, we obtain the following MIMO system

$$\dot{\mathbf{x}}_t = A\mathbf{x}_t + B\mathbf{u}, \tag{4}$$

where $\mathbf{x}_t = [x_1 \ \dot{x}_1 \ \cdots \ x_N \ \dot{x}_N]^T$ is the state vector, $\mathbf{u} = [u_1 \ \cdots \ u_N]^T$ the control input vector, $A \in \mathbb{R}^{kN\times kN}$ a matrix of unknown parameters, $B \in \mathbb{R}^{kN\times N}$ a known matrix and k the number of states per direction, here $k = 2$. More specifically, the A and B are defined by $A = \left[A_{ji}\right]_{N\times N}$ where

$$A_{jj} = \begin{bmatrix} 0 & 1 \\ a_{jj,1} & a_{jj,2} \end{bmatrix} \text{ and } A_{ji} = \begin{bmatrix} 0 & 0 \\ a_{ji,1} & a_{ji,2} \end{bmatrix} \text{ for } j \neq i$$

where $a_{jj,1} = -(k_{P_{jj}} + k_e)$, $a_{jj,2} = -(k_{D_{jj}} + d_e)$, $a_{ji,1} = -k_{P_{ji}}$, $a_{ji,2} = -k_{D_{ji}}$, $i, j = 1, ..., N, i \neq j$ and

$$B = diag(\mathbf{b}_1, \cdots, \mathbf{b}_N), \quad \mathbf{b}_i = \begin{bmatrix} 0 \\ 1 \end{bmatrix}.$$

B. Problem definition

As it is analyzed in section II-A, the end-effector motion dynamics are given by (4). We assume that a reference model exists, which expresses the desired response of the system to a reference signal $\mathbf{r}$, and has the form

$$\dot{\mathbf{x}}_t^* = A^*\mathbf{x}_t^* + B^*\mathbf{r} \tag{5}$$

where $\mathbf{x}_t^* = [x_1^* \ \dot{x}_1^* \ \cdots \ x_N^* \ \dot{x}_N^*]^T \in \mathbb{R}^{kN}$ is the reference state vector, x_i^* is the reference position, $A^* \in \mathbb{R}^{kN\times kN}$ and $B^* \in \mathbb{R}^{kN\times N}$ are known matrices and $\mathbf{r} = [r_1 \ \cdots \ r_N]^T$.

Our goal is to design a control law $\mathbf{u}$ in (4) such that the state vector $\mathbf{x}_t$ globally and asymptotically tracks the reference state vector $\mathbf{x}_t^*$ by minimizing, in each direction, the cost

$$J = J_1 + ... + J_N$$

where J_i is a function of the motion states of the i-th direction. In this way, we aim at individual state tracking in each direction by simultaneously taking into account the state tracking error of all the directions of the workspace. Given the directional physical coupling, control of motion in one direction should not be realized independently of the motion control in all other directions since this may violate the physical constraints of the system.

III. Main results

To solve our problem, we develop a MIMO adaptive control approach which combines MRAC with ESC.

For the remainder of the paper, for the sake of simplicity and without loss of generality, we assume that the end-effector interacts with the environment in two directions of movement only, i.e. $N = 2$.

A. MRAC and ESC principle

Fig. 2 illustrates the ESC-MRAC principle for a SISO system which operates in the i-th movement direction. MRAC expresses the system's desired response to a reference signal r_i in terms of a reference model, see Fig. 2(a). In state tracking, the objective consists of designing the

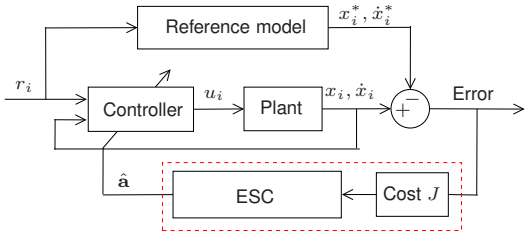

(a) ESC-MRAC

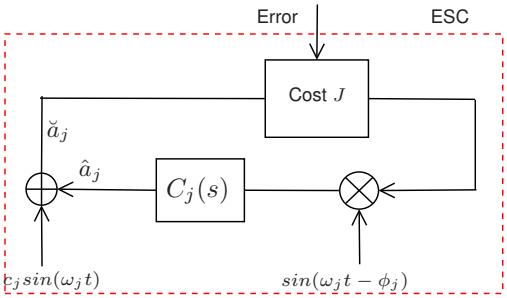

(b) ESC

Fig. 2. (a) ESC-MRAC block diagram of a SISO system in the i-th movement direction. The plant's state vector $[x_i \ \dot{x}_i]$ is ensured to track the reference state vector $[x_i^* \ \dot{x}_i^*]$ through appropriate design of the control law u_i. The parameter vector $\hat{\mathbf{a}} = \{\hat{a}_j\}$ of the controller is updated based on the minimization of the cost J through ESC. (b) ESC diagram. The ESC loop is realized for every single parameter a_j of the system.

control law u_i such that the error $[x_i \ \dot{x}_i]^T - [x_i^* \ \dot{x}_i^*]^T$ converges to zero. In ESC, the parameters of the control law are adjusted while seeking the extremum of a cost criterion J [5], [9]. The most common technique is the Perturbation-based ESC (PESC) because of its simple implementation and fast convergence compared to other ESC techniques. PESC is a gradient-based optimization technique where a sinusoidal perturbation $c_j sin(\omega_j t)$ is used to update the estimates $\hat{a}_j$ of the control parameters a_j at each iteration, see Fig. 2(b). Analytical explanation of how ESC works can be found in [5], [9].

B. MIMO ESC-MRAC

In this section, we develop an ESC-MRAC scheme for state tracking in linear MIMO systems where PESC is used. Our approach is inspired by [10].

1) Motion dynamics: We consider the two subsystems

$$\begin{aligned} a_2\ddot{x}_1 + a_1\dot{x}_1 + a_0 x_1 + a_3 x_2 + a_4\dot{x}_2 = u_1, \\ a_7\ddot{x}_2 + a_6\dot{x}_2 + a_5 x_2 + a_8 x_1 + a_9\dot{x}_1 = u_2, \end{aligned} \tag{6}$$

where $x_i, \dot{x}_i, \ddot{x}_i, \ i = 1, 2$ are measurable states, x_i represents position and a_j are unknown parameters. Correspondingly to (6), the reference model has the form

$$\begin{aligned} a_2^*\ddot{x}_1^* + a_1^*\dot{x}_1^* + a_0^* x_1^* + a_3^* x_2^* + a_4^*\dot{x}_2^* = r_1, \\ a_7^*\ddot{x}_2^* + a_6^*\dot{x}_2^* + a_5^* x_2^* + a_8^* x_1^* + a_9^*\dot{x}_1^* = r_2. \end{aligned} \tag{7}$$

The goal consists of designing a control law $\mathbf{u} = [u_1 \ u_2]^T$ such that the error $\mathbf{e} = [e_1 \ \dot{e}_1 \ e_2 \ \dot{e}_2]^T$ converges to zero where $e_1 = x_1 - x_1^*$ and $e_2 = x_2 - x_2^*$. We define the control signals as

$$\begin{aligned} u_1 = \breve{a}_2 z_1 + \breve{a}_1\dot{x}_1 + \breve{a}_0 x_1 + \breve{a}_3 x_2 + \breve{a}_4\dot{x}_2, \\ u_2 = \breve{a}_7 z_2 + \breve{a}_6\dot{x}_2 + \breve{a}_5 x_2 + \breve{a}_8 x_1 + \breve{a}_9\dot{x}_1. \end{aligned} \tag{8}$$

The parameters $\breve{a}_i$ are updated according to $\breve{a}_j = \hat{a}_j + c_j sin\omega_j t$, see Fig. 2. The parameter error is defined as $\tilde{a}_j = a_j - \hat{a}_j$. The signals z_i are defined as

$$\begin{aligned} z_1 = \ddot{x}_1^* - \beta_0 e_1 - \beta_1\dot{e}_1 - \beta_2 e_2 - \beta_3\dot{e}_2, \\ z_2 = \ddot{x}_2^* - \beta_4 e_2 - \beta_5\dot{e}_2 - \beta_6 e_1 - \beta_7\dot{e}_1 \end{aligned} \tag{9}$$

where β_i are known parameters.

2) Dynamics of state tracking and parameter error: Fig. 2(b) illustrates the PESC parameter adaptation law which is employed for the update of the $\breve{a}_0, ..., \breve{a}_9$ parameters. The compensator $C_j(s)$ in Fig. 2 is defined as [10]

$$C_j(s) = -g_j\left(\frac{1 + d_j s}{s}\right) \tag{10}$$

where $g_j, \ d_j \in \mathbb{R}$ are known parameters and s the complex Laplace variable. Based on Fig. 2(b), the dynamics of the parameter error are

$$\dot{\tilde{a}}_j = -\dot{\hat{a}}_j = g_j(1 + d_j s)\ [sin(\omega_j t - \phi_j)J(t)] \tag{11}$$

which can be written as

$$\begin{aligned} \dot{\tilde{a}}_j = g_j\left(sin(\omega_j t - \phi_j) + d_j\omega_j cos(\omega_j t - \phi_j)\right) J(t) + \\ g_j d_j sin(\omega_j t - \phi_j)\dot{J}(t) \end{aligned} \tag{12}$$

where $j = 0, ..., 9$. The cost function is defined by

$$\begin{aligned} J = (Q_1\mathbf{e})^T(Q_1\mathbf{e}), \\ Q_1 = \begin{bmatrix} q_1 & q_2 & 0 & 0 \\ 0 & 0 & q_3 & q_4 \end{bmatrix} \end{aligned} \tag{13}$$

where $q_1, \ q_2, \ q_3, \ q_4$ are known, real-valued parameters. By combining all $\dot{\tilde{a}}_j$ from (12), we can write

$$\dot{\tilde{\mathbf{a}}} = G\mathbf{l}J + G\mathbf{m}\dot{J} \tag{14}$$

where $\mathbf{l} = \begin{bmatrix} l_0 & \cdots & l_9 \end{bmatrix}^T$, $\mathbf{m} = \begin{bmatrix} m_0 & \cdots & m_9 \end{bmatrix}^T$,

$$l_j = sin(\omega_j t - \phi_j) + d_j\omega_j cos(\omega_j t - \phi_j),$$

$$m_j = d_j \ sin(\omega_j t - \phi_j),$$

$G = diag([g_j]) \in \mathbb{R}^{10\times 10}$ and $\tilde{\mathbf{a}} = [\tilde{a}_0 \cdots \tilde{a}_9]^T \in \mathbb{R}^{10}$. By combining (6) with (8)-(9), we infer the tracking error dynamics

$$\begin{aligned} \ddot{e}_1 + \beta_0 e_1 + \beta_1\dot{e}_1 + \beta_2 e_2 + \beta_3\dot{e}_2 = \frac{1}{a_2}((p_2 - \tilde{a}_2)z_1 + (p_0 - \tilde{a}_0)x_1 \\ + (p_1 - \tilde{a}_1)\dot{x}_1 + (p_3 - \tilde{a}_3)x_2 + (p_4 - \tilde{a}_4)\dot{x}_2), \end{aligned} \tag{15}$$

$$\begin{aligned} \ddot{e}_2 + \beta_4 e_2 + \beta_5\dot{e}_2 + \beta_6 e_1 + \beta_7\dot{e}_1 = \frac{1}{a_7}((p_7 - \tilde{a}_7)z_2 + (p_5 - \tilde{a}_5)x_2 \\ + (p_6 - \tilde{a}_6)\dot{x}_2 + (p_8 - \tilde{a}_8)x_1 + (p_9 - \tilde{a}_9)\dot{x}_1), \end{aligned} \tag{16}$$

where $p_i = c_i sin\omega_i t$. The $e_i, \dot{e}_i, \ddot{e}_i$ represent the position, velocity and acceleration error respectively. By combining (15)-(16), we write the total tracking error dynamics as

$$\dot{\mathbf{e}} = E\mathbf{e} + B_e P^*\mathbf{v} \tag{17}$$

where $\mathbf{v} = \begin{bmatrix} x_1 & \dot{x}_1 & z_1 & x_2 & \dot{x}_2 & z_2 \end{bmatrix}^T$, $P^* = P - \tilde{A}$,

$$E = \begin{bmatrix} 0 & 1 & 0 & 0 \\ -\beta_0 & -\beta_1 & -\beta_2 & -\beta_3 \\ 0 & 0 & 0 & 1 \\ -\beta_6 & -\beta_7 & -\beta_4 & -\beta_5 \end{bmatrix}, \quad B_e = \begin{bmatrix} 0 & 0 \\ \frac{1}{a_2} & 0 \\ 0 & 0 \\ 0 & \frac{1}{a_7} \end{bmatrix},$$
$$\tilde{A} = \begin{bmatrix} \tilde{a}_0 & \tilde{a}_1 & \tilde{a}_2 & \tilde{a}_3 & \tilde{a}_4 & 0 \\ \tilde{a}_8 & \tilde{a}_9 & 0 & \tilde{a}_5 & \tilde{a}_6 & \tilde{a}_7 \end{bmatrix}, \quad (18)$$
$$P = \begin{bmatrix} p_0 & p_1 & p_2 & p_3 & p_4 & 0 \\ p_8 & p_9 & 0 & p_5 & p_6 & p_7 \end{bmatrix}.$$

Theorem 1. *Consider the system* (6) *whose control law is given by* (8)-(9)*, parameter error dynamics are governed by* (14)*, the cost function J is given by* (13) *and the compensator $C(s)$ by* (10)*. Then, there exist parameters d_i, g_i, ω_i, β_i, ϕ_i and c_i such that the error* $\mathbf{e}$ *globally and asymptotically converges to zero, where $\omega_i \geq 1$, $\omega_i \in \mathbb{N}$.*

Proof. We define the augmented state vector $\mathbf{y} = [\mathbf{e}\ \tilde{\mathbf{a}}]^T$ where

$$\dot{\mathbf{y}} = f(t, \mathbf{y}) = \begin{bmatrix} E\mathbf{e} + B_e P^* \mathbf{v} \\ G\mathbf{l}J + G\mathbf{m}\dot{J} \end{bmatrix}. \quad (19)$$

To deal with non-autonomous system (19), we follow the approach of averaging [15]. Averaging applies on systems of the form $\dot{\mathbf{y}} = \epsilon f(t, \mathbf{y})$ and, to make (19) in this form, we perform scaling by setting $t = \epsilon\tau$ where ϵ is a small positive parameter. We denote the average by $AVG(\cdot)$ or, for reasons of convenience, for single-term arguments by $(\cdot)_{av} = AVG(\cdot)$. Based on this, we have

$$\frac{d\mathbf{y}}{d\tau} = \epsilon f(\tau, \mathbf{y}), \quad (20)$$
$$\frac{d\mathbf{y}}{d\tau} = \epsilon f_{av}(\mathbf{y}). \quad (21)$$

According to the averaging theorem, given specific conditions, the solution of (20) can be approximated by the solution of its average system (21), that is, there exist $\epsilon^* > 0$ such that for all $0 < \epsilon < \epsilon^*$, it is

$$\mathbf{y}(\tau, \epsilon) - \mathbf{y}_{av}(\epsilon\tau) = O(\epsilon) \text{ for all } t \in [0, \infty) \quad (22)$$

where $\mathbf{y}$ and $\mathbf{y}_{av}$ are solutions of (20) and (21) respectively. Here, we do not analyze the conditions of the averaging theorem due to space limitations. The average tracking error dynamics can be written as

$$\dot{\mathbf{e}}_{av} = E\mathbf{e}_{av} - B_e \tilde{A}_{av} \mathbf{v}_{av} \quad (23)$$

given that P, $\tilde{A}$, $\mathbf{v}$ are uncorrelated and $P_{av} = [0] \in \mathbb{R}^{2\times 6}$. The average parameter error dynamics can be written as

$$\dot{\tilde{\mathbf{a}}}_{av} = 2\ AVG(G\mathbf{m}\mathbf{e}^T Q B_e P)\mathbf{v}_{av} \quad (24)$$

where $Q = Q_1^T Q_1$, given that $\mathbf{l}_{av} = \mathbf{m}_{av} = \mathbf{0} \in \mathbb{R}^{10}$. Let us consider the Lyapunov candidate function

$$V = \mathbf{e}_{av}^T P_1 \mathbf{e}_{av} + \tilde{\mathbf{a}}_{av}^T P_2 \tilde{\mathbf{a}}_{av}$$

where $P_1 \in \mathbb{R}^{4\times 4}$ and $P_2 \in \mathbb{R}^{10\times 10}$ are symmetric positive definite matrices. By computing the derivative of V and substituting dynamics (23) into $\dot{V}$, we have

$$\dot{V} = \mathbf{e}_{av}^T(-L)\mathbf{e}_{av} - 2\mathbf{v}_{av}^T \tilde{A}_{av}^T B_e^T P_1 \mathbf{e}_{av} + 2\tilde{\mathbf{a}}_{av}^T P_2 \dot{\tilde{\mathbf{a}}}_{av} \quad (25)$$

where $-L = E^T P_1 + P_1 E$ and L is a positive definite matrix. It is $\dot{V} \leq 0$ if

$$\mathbf{v}_{av}^T \tilde{A}_{av}^T B_e^T P_1 \mathbf{e}_{av} = \tilde{\mathbf{a}}_{av}^T P_2 \dot{\tilde{\mathbf{a}}}_{av}. \quad (26)$$

By substituting dynamics (24) into condition (26), the condition can be equivalently written as

$$\tilde{A}_{av}^T B_e^T P_1 \mathbf{e}_{av} = 2(AVG(\mathbf{m}_g \mathbf{e}^T Q^*))^T P_2 \tilde{\mathbf{a}}_{av} \quad (27)$$

where $\mathbf{m}_g = [g_i m_i] \in \mathbb{R}^{10}$ and $Q^* = QB_eP$. We denote by $\mathbf{1}_n$ and $\mathbf{0}_n$ the row vectors of all ones and all zeros respectively, with dimension $1 \times n$. We express $\tilde{A}_{av} = A_s diag(\tilde{\mathbf{a}}_{av}) B_s$ and $\tilde{\mathbf{a}}_{av} = diag(\tilde{\mathbf{a}}_{av})(\mathbf{1}_{10})^T$ where

$$A_s = \begin{bmatrix} \mathbf{1}_5 & \mathbf{0}_5 \\ \mathbf{0}_5 & \mathbf{1}_5 \end{bmatrix}, \ B_s = \begin{bmatrix} 1 & 0 & 0 & 0 & 0 & 0 \\ 0 & 1 & 0 & 0 & 0 & 0 \\ 0 & 0 & 1 & 0 & 0 & 0 \\ 0 & 0 & 0 & 1 & 0 & 0 \\ 0 & 0 & 0 & 0 & 1 & 0 \\ 0 & 0 & 0 & 1 & 0 & 0 \\ 0 & 0 & 0 & 0 & 1 & 0 \\ 0 & 0 & 0 & 0 & 0 & 1 \\ 1 & 0 & 0 & 0 & 0 & 0 \\ 0 & 1 & 0 & 0 & 0 & 0 \end{bmatrix}.$$

Based on these expressions and after a series of algebraic calculations, (27) becomes

$$\mathbf{w}_2 A_s^T B_e^T P_1 = 2\mathbf{w}_1 (AVG(fQ^*))^T \quad (28)$$

where $\mathbf{w}_1 = \mathbf{1}_6$, $\mathbf{w}_2 \in \mathbb{R}^{1\times 10}$ is a known constant vector which can be defined by the user and $f = \mathbf{w}_2 P_2 \mathbf{m}_g$. Given condition (28), $\dot{V}$ becomes

$$\dot{V} = \mathbf{e}_{av}^T(-L)\mathbf{e}_{av} \leq 0, \quad (29)$$

and, thus, $\mathbf{e}_{av}$, $\tilde{\mathbf{a}}_{av}$ and, in turn, $\mathbf{v}_{av}$ are bounded. Therefore, $\ddot{V} = -\mathbf{e}_{av}^T(E^T L + LE)\mathbf{e}_{av} + \mathbf{e}_{av}^T(L^T + L)B_e \tilde{A}_{av}\mathbf{v}_{av}$ is also bounded. Based on Barbalat's lemma, we have $\lim_{t\to\infty} \dot{V} = 0$, and from (29), $\lim_{t\to\infty} \mathbf{e}_{av} = 0$. Given that $\tilde{\mathbf{a}}_{av}$ is bounded and, that from (25) for $\mathbf{e}_{av} \to \infty$ the $V \to \infty$, the $\mathbf{e}_{av}$ globally and asymptotically converges to zero [15]. The condition $\omega_i \geq 1$, $\omega_i \in \mathbb{N}$ comes from the satisfaction of the conditions of the averaging theorem. □

3) Setting the parameters: (i) Set β_i such that E is Hurwitz, (ii) compute P_1 from $E^T P_1 + P_1 E = -L$, here we set $L = diag([1\ 1\ 1\ 1])$, (iii) set q_i as desired, (iv) tune g_i, c_i, ϕ_i and parameters of P_2 such that they satisfy condition (28). The c_i should be relatively large such that they cause noticeable perturbations to the system. Large g_i can increase the rate of change of the parameters while large values of P_2 parameters may decrease the parameter adaptation rate [10].

IV. Evaluation

The proposed MIMO ESC-MRAC is evaluated in simulation and compared with SISO ESC-MRAC [10] in a real-world robotic engraving experiment.

A. Simulation

Here, we evaluate the performance of the currently proposed MIMO ESC-MRAC approach in simulation. Let us

assume a robot end-effector which moves in 2 directions, which we call normal and parallel. The system dynamics are given by (4) where $\mathbf{x}_t = [x_1\ \dot{x}_1\ x_2\ \dot{x}_2]^T$ and

$$A = \begin{bmatrix} 0 & 1 & 0 & 0 \\ -3.6 & -2 & -1.2 & -1.4 \\ 0 & 0 & 0 & 1 \\ -2.25 & -1.25 & -3.75 & -2.5 \end{bmatrix}, \quad B = \begin{bmatrix} 0 & 0 \\ 1 & 0 \\ 0 & 0 \\ 0 & 1 \end{bmatrix}.$$

The reference model is given by (5) where

$$A^* = \begin{bmatrix} 0 & 1 & 0 & 0 \\ -15 & -11.25 & -1.2 & -1.6 \\ 0 & 0 & 0 & 1 \\ -2 & -3 & -2 & -3 \end{bmatrix}, \quad B^* = B,$$

$\mathbf{x}_t^* = [x_1^*\ \dot{x}_1^*\ x_2^*\ \dot{x}_2^*]^T$, $\mathbf{r} = [r_1\ r_2]^T$ and r_1 and r_2 are reference signals of the normal and parallel direction. The A^* is set such that x_1^* and x_2^* track r_1 and r_2 respectively. The reference signals are acquired through demonstration of an engraving task on the plasticine material of Fig. 4.

The goal consists of making $\mathbf{x}_t$ track $\mathbf{x}_t^*$. Fig. 3 shows tracking of reference position x_1^*, x_2^* and velocity $\dot{x}_1^*$, $\dot{x}_2^*$ states by the system's position x_1, x_2 and velocity $\dot{x}_1$, $\dot{x}_2$ states respectively as well as the corresponding tracking error in both directions, by using MIMO ESC-MRAC. We observe that, although the position tracking error is relatively high during the first few seconds of the task and approaches the value of 1mm, this error converges rather fast to zero afterwards. The same occurs with the velocity tracking error which initially approaches the 2mm/s and converges fast to zero after 1 second. For the simulation, we set $\omega_0 = 100$, $\omega_1 = 8$, $\omega_2 = \omega_7 = 14$, $\omega_3 = 110$, $\omega_4 = 85$, $\omega_5 = 15$, $\omega_6 = 8$, $\omega_8 = 60$, $\omega_9 = 50$ and $c_0 = 0.3$, $c_1 = c_2 = c_3 = c_4 = c_5 = c_6 = c_7 = c_8 = c_9 = 0.2$.

B. Experimental evaluation

We evaluate proposed MIMO ESC-MRAC in a real-world robotic engraving task by using a 2-DoF linear-actuated haptic device (*ThrustTube*), see Fig. 4. A force/torque sensor measures the end-effector force and device's encoders measure end-effector position and velocity. The end-effector can move in two directions, one normal and one parallel to the object's initially planar surface. A sculpting tool is firmly attached on the end-effector for engraving and the system end-effector - tool behaves as a rigid body.

Prior to the task, the end-effector is placed such that the tool tip just touches the object's surface. The end-effector is commanded to follow a reference motion in the two directions while the tool engraves a pattern into the plasticine material. For our task, we employ a controller which consists of the superposition of adaptive ESC-MRAC and fixed-gain positional control. The haptic device involves some friction and the positional control compensates for this friction while ESC-MRAC compensates for the system uncertainty during the interaction of the end-effector with the environment.

Fig. 5 shows execution of a motion by applying MIMO ESC-MRAC and SISO ESC-MRAC [10]. The parameters of the reference models in both approaches are set such that the reference position states track the reference signals, see

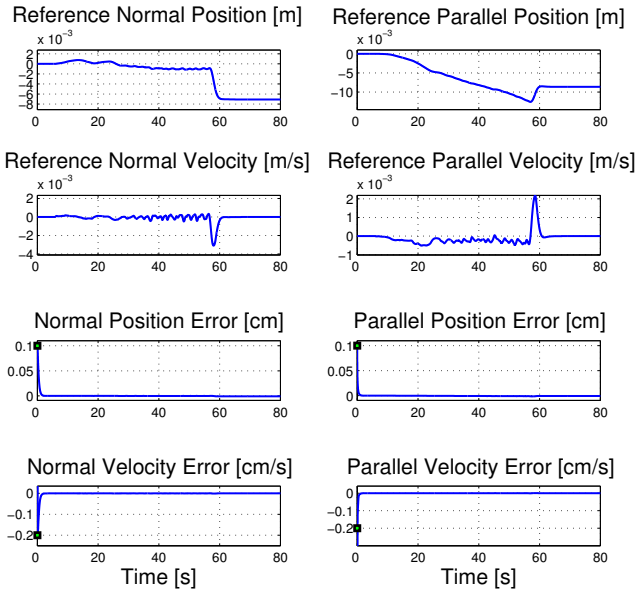

Fig. 3. State tracking by proposed MIMO ESC-MRAC: (top raw) reference position, (second raw) reference velocity, (third raw) position tracking error, (bottom raw) velocity tracking error. Markers are used to highlight the initial error value. The position and velocity signals are expressed in m and m/s respectively while the corresponding tracking errors are expressed in cm and cm/s respectively. All signals are expressed with respect to time in sec.

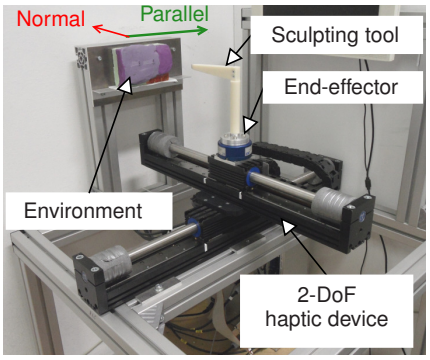

Fig. 4. Experimental setup. The two directions of movement, normal and parallel, are visualized by a red- and a green-color axis respectively.

Fig. 5(a),(b). The parameters of the cost functions J_1 and J_2 are set $q_1 = -1.52$, $q_2 = 12.79$, $q_3 = 23.44$ and $q_4 = 7.82$. In case of SISO ESC-MRAC, the two directions of movement are treated as two independent SISO systems and systems' parameters are tuned, according to [10], to achieve optimal performance. In MIMO ESC-MRAC, the c_i signals are $c_0 = 3$, $c_1 = c_2 = c_7 = 2$, $c_3 = c_8 = 30$, $c_4 = c_9 = 30$, $c_5 = 21$, $c_6 = 5$ and the frequencies are $\omega_0 = 100$, $\omega_1 = 8$, $\omega_2 = 14$, $\omega_3 = 10$, $\omega_4 = 5$, $\omega_5 = 230$, $\omega_6 = 150$, $\omega_7 = 120$, $\omega_8 = 40$, $\omega_9 = 50$.

Fig. 5(a) refers to MIMO ESC-MRAC while Fig. 5(b) to SISO ESC-MRAC. We define the tracking error as the difference between the reference and measured position. Fig. 5(c) shows the tracking error in the two directions of movement for MIMO ESC-MRAC and SISO ESC-MRAC. The position signals are of order $10^{-3}m$ in the normal direction and $10^{-2}m$ in the parallel direction while the

tracking errors are of order $10^{-4}m$. We observe that MIMO ESC-MRAC exhibits lower transient and steady-state error compared to SISO ESC-MRAC. In MIMO ESC-MRAC, a rather low steady-state error almost equal to $10^{-4}m$ exists, which may be due to non-modelled inherent end-effector dynamics. This error could be potentially eliminated by combining with some integral control.

V. Conclusion

In this work, we present a MIMO ESC-MRAC approach for realization of multi-directional constrained robotic motion tasks in presence of uncertainty. The proposed method achieves state tracking as well as optimization of a global state-dependent cost criterion in all directions of movement simultaneously.

ACKNOWLEDGMENT

This research has been partially supported by TUM-Institute for Advanced Study and the scholarship 'TUM-Chancengleichheit fuer Frauen in Forschung und Lehre'.

References

[1] J. Peters and S. Schaal. Learning to control in operational space, *International Journal of Robotics Research*, 27(2), pp.197-212, 2008.
[2] D. Mitrovic, S. Klanke and S. Vijayakumar, Adaptive optimal feedback control with learned internal dynamics models, *From Motor Learning to Interaction Learning in Robots*, SCI 264, pp. 65-84, Springer-Verlag, 2010.
[3] V. Koropouli, S. Hirche and D. Lee, Learning and generalizing force control policies for sculpting, *Intelligent Robots and Systems (IROS)*, pp.1493-1498, 2012.
[4] J.R. Medina Hernndez, Dongheui Lee, S. Hirche, Risk-sensitive optimal feedback control for haptic assistance, *IEEE International Conference on Robotics and Automation (ICRA)*, 2012 .
[5] C. Zhang and R. Ordez, Extremum-Seeking Control and Applications, New York: Springer, 2012.
[6] K. S. Narendra and A. M. Annaswamy, Stable adaptive systems, New York: Dover Publications, 2005.
[7] K. J. Astrom, B. Wittenmark, Adaptive control, New York: Dover Publications, 2008.
[8] J. X. Guo, Y. Liu, and G. Tao, Multivariable MRAC with state feedback for output tracking, *Proceedings of the American Control Conference*, pp. 592-597, 2009.
[9] B. K. Ariyur and M. Krstic, Real-Time Optimization by Extremum-Seeking Control, Wiley, 2003.
[10] H. Poorya and K.B. Ariyur, ES-MRAC: A New Paradigm For Adaptive Control, arXiv:1207.5642, July 2012.
[11] P. Haghi and K.B. Ariyur, On the extremum seeking of model reference adaptive control in higher-dimensional systems, *Proceedings of the American Control Conference*, pp. 1176-1181, 2011.
[12] N. Hogan, Impedance control: An approach to manipulation: Parts I-III, *Journal of Dynamic Systems, Measurement and Control*, vol. 107, pp. 1-24, 1985.
[13] C. Ott, Cartesian impedance control of redundant and flexible-joint robots, Berlin: Springer, 2008.
[14] L. Sciavicco and B. Siciliano, Modeling and Control of Robot Manipulators, McGraw-Hill, 1996.
[15] H.K.Khalil, Nonlinear systems, 3rd edition, New Jersey: Prentice Hall, 2002.
[16] P. Haghi and K.B.Ariyur, Adaptive feedback linearization of nonlinear MIMO systems using ES-MRAC, *American Control Conference*, pp. 1828-1833, 2013.

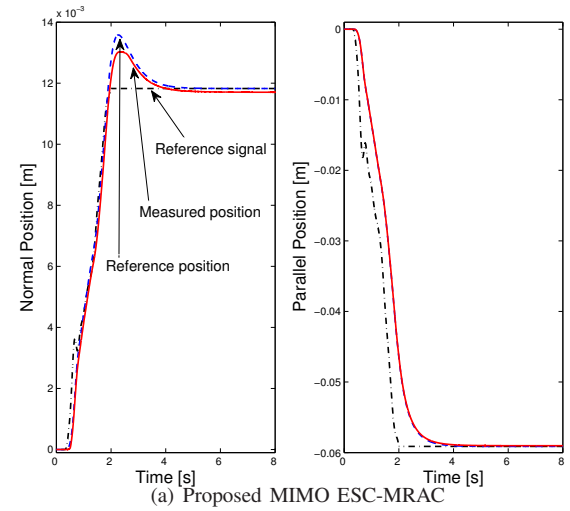

(a) Proposed MIMO ESC-MRAC

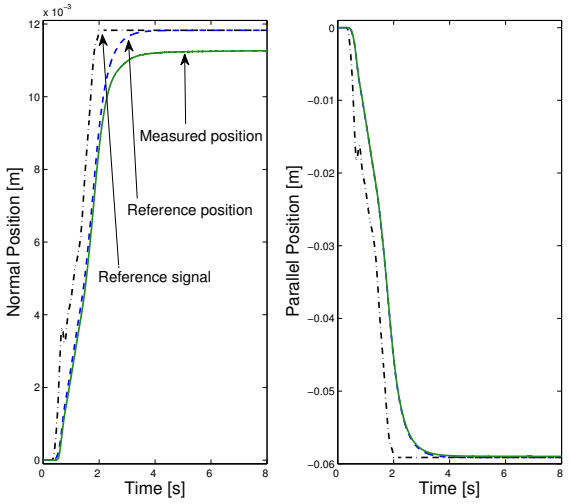

(b) SISO ESC-MRAC

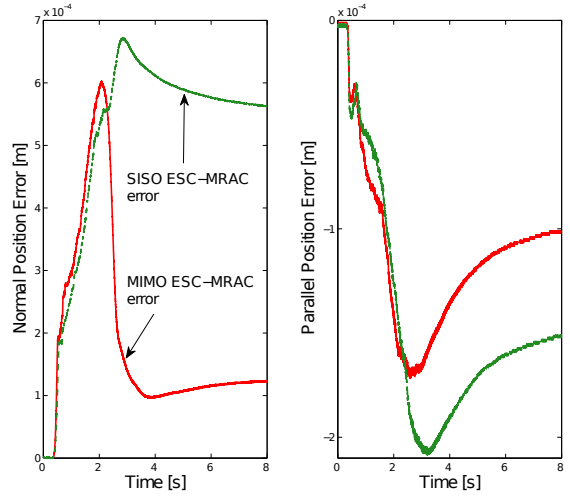

(c) Tracking error of MIMO ESC-MRAC and SISO ESC-MRAC

Fig. 5. Motion tracking by (a) proposed MIMO ESC-MRAC: (dash-dot black line) reference signal, (dashed blue line) reference position, (solid red line) measured position, (b) SISO ESC-MRAC: (dash-dot black line) reference signal, (dashed blue line) reference position, (solid green line) measured position. (c) Error between the reference and measured position of: (solid red line) MIMO ESC-MRAC, (dashed green line) SISO ESC-MRAC.